Reactive and Functional Polymers 205 (2024) 106085

Contents lists available at ScienceDirect

Reactive and Functional Polymers

journal homepage: www.elsevier.com/locate/react

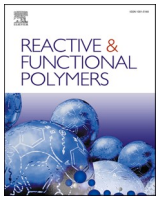

Design of photocurable thiol-epoxy resins for the processing of vitrimers with vat photopolymerisation 3D printing

Szymon Gaca [a,b], Kurt Dietliker [c], Elisabeth Rossegger [a], Sandra Schlögl [a,b,*]

[a] Polymer Competence Center Leoben GmbH, Sauraugasse 1, 8700 Leoben, Austria
[b] Chair of Chemistry of Polymeric Materials, Montanuniversitaet Leoben, Otto Glöckel-Straße 2/IV, 8700 Leoben, Austria
[c] SCD Dr. Sommerlade Chemistry Design GmbH, Rheinfeldener Straße 27, 79395 Neuenburg am Rhein, Germany

ARTICLE INFO

Keywords:
Digital light processing 3D printing
Thiol-epoxy resins
Anionic photocuring
Vitrimers
Photobase generator

ABSTRACT

Vat photopolymerisation 3D printing is a convenient approach to fabricating complex polymeric objects based on the localised photocuring of a liquid resin. Advancing from free-radical mediated curing mechanisms, the current study focuses on the vat photopolymerisation 3D printing of photopolymers formed by an ionic click reaction between thiol and epoxy monomers. In this process, selected epoxy monomers are mixed with a tetra-functional thiol crosslinker and a photobase generator, which releases 1,5-diazabicyclo[4.3.0]non-5-ene (DBN) upon light exposure to initiate the anionic ring-opening reaction. FTIR, photo-DSC and rheology studies reveal a slow cure rate of the thiol-epoxy resins at room temperature, which is significantly accelerated by increasing the temperature to 50 °C during light irradiation. By optimising the resin composition, shelf life and viscosity, printing of objects via digital light processing 3D printing is enabled by using a vat heated to 50 °C. The printed thiol-epoxy networks contain ample -OH and ester moieties, which undergo thermo-activated bond exchange reactions. Here, the photochemically liberated DBN molecules act as catalysts to accelerate the transesterification reaction at elevated temperatures (150–180 °C). Rheological measurements demonstrate the efficient and Arrhenius-like behaviour of the networks' stress relaxation, giving rise to the dynamic nature of the printed photopolymers, which is further confirmed by reshaping experiments.

1. Introduction

Additive manufacturing (AM) has gained widespread interest in recent years, as it allows the fabrication of complex objects without the need for expensive moulds used in injection moulding or the requirement for energy- and time-consuming post-processing steps [1]. Among the various AM techniques, vat photopolymerisation 3D printing stands out due to the high resolution and surface quality of the printed parts, along with the decent build speed [2]. In particular, vat photopolymerisation 3D printing relies on the spatially controlled solidification of a liquid resin in a vat through selective light exposure. In digital light processing (DLP) 3D printing, photopolymerisation occurs layer-by-layer, significantly accelerating the build speed of the objects. Moreover, DLP 3D printing does not require the high temperatures used in fused filament fabrication (FFF), making it economical and suitable for the processing of temperature-sensitive materials. Additionally, printing with liquid resins offers a wide range of possibilities for combining different materials and incorporating selected fillers [3–5]. Due to these advantages, DLP 3D printing is employed in numerous application fields, including (micro)electronics, rapid prototyping, dentistry, and art [6,7].

Commercially available resins for DLP 3D printing are primarily based on photocurable (meth)acrylates [8], which are cured by radical-mediated chain growth polymerisation. This diffusion-controlled curing mechanism typically yields photopolymers with low final monomer conversion, high shrinkage, and internal stress, negatively affecting the accuracy and mechanical properties of the cured objects [9]. One approach to overcome shrinkage stress is the use of resins that are photocured by a step-growth mechanism, such as thiol-ene click chemistry [10]. In this process, thiols are added as crosslinking agents to (meth) acrylates and alkenes to shift the gel point to higher conversions, resulting in photopolymers with high network homogeneity. Click reactions are organic reactions characterised by excellent conversion, stereoselectivity, and a high reaction rate under mild conditions. For

* Corresponding author at: Polymer Competence Center Leoben GmbH, Sauraugasse 1, 8700 Leoben, Austria; Chair of Chemistry of Polymeric Materials, Montanuniversitaet Leoben, Otto Glöckel-Straße 2/IV, 8700 Leoben, Austria.
E-mail addresses: sandra.schloegl@pccl.at, sandra.schloegl@unileoben.ac.at (S. Schlögl).

https://doi.org/10.1016/j.reactfunctpolym.2024.106085
Received 8 September 2024; Received in revised form 26 October 2024; Accepted 29 October 2024
Available online 30 October 2024

DLP 3D printing, thiol-ene [11–14], thiol-yne [15–17], and the cationic ring-opening reaction of epoxies have been utilised, all of which fulfill the characteristics of click chemistry [18].

However, click reactions following an anionic curing mechanism are still underexplored for vat photopolymerisation 3D printing, primarily due to their slow reaction rate. One example is the base-catalysed ring-opening reaction between epoxy and thiol groups (Fig. 1). In the first step of this reaction, the thiol groups are deprotonated in the presence of a strong base, yielding thiolates, which react with the epoxy groups via nucleophilic ring-opening. As thiolates are stronger nucleophiles than alkoxides, the reaction follows a step-growth mechanism, whilst homopolymerisation of the epoxy groups does not play a significant role [19]. To ensure spatial and temporal control of the reaction, photobase generators (PBGs) are added to the thiol-epoxy resins. Once activated upon light exposure, the PBG releases a strong base capable of deprotonating the thiol and initiating the curing reactions [20].

Over the past few years, the light-triggered thiol-epoxy reaction has primarily been applied in the preparation of functional coatings. Bouzrati-Zerelli et al. described the light-activated curing of thiol-epoxy resins, which benefit from a high final monomer conversion. However, the resins suffered from a slow cure reaction, taking 90 min to reach final monomer conversion [21]. Pursuing a similar strategy, Chen et al. proposed the use of a PBG to retard the thiol-epoxy crosslinking reaction, allowing the resin components to be fully mixed without the risk of premature gelation [22]. Along with the long reaction time, the authors encountered other challenges, such as the need to use solvents to adjust the resin's viscosity. To accelerate the cure kinetics of the thiol-epoxy resins, Jian et al. used a mixture of epoxy and acrylic resins but noted that the hybrid resin exhibited a poor shelf life [23]. Due to the lack of available resins combining rapid curing with high shelf life and low viscosity, to the best of our knowledge, no work has yet been published on the processing of thiol-epoxy systems with DLP 3D printing.

To tackle this challenge, the current study focuses on the development of DLP 3D printable thiol-epoxy resins, which provide a sufficiently shelf life (at temperatures up to 50 °C), adequate cure rate and conversion, good miscibility, and low viscosity. The aforementioned studies have been used as a starting point, describing the use of bisphenol A diglycidyl ether (DGEBA) and 3,4-epoxycyclohexylmethyl-3′,4′-epoxycyclohexane carboxylate (ECC) with varying reactivity in the thiol-epoxy reaction. Herein, a tetra-functional thiol is used as a crosslinker to ensure a high crosslink density in the printed objects. A commercially available PBG (SCD-PLB-090) was utilised, which liberates 1,5-diazabicyclo[4.3.0]non-5-ene (DBN) upon irradiation with UV light. By optimising the composition, a resin is obtained which is processable by DLP 3D printing at 50 °C. As the cured network provides ample -OH (formed by the ring-opening reaction) and ester (introduced by the choice of crosslinker) groups, the printed objects are able to undergo base-catalysed transesterification reactions in the presence of the released DBN. The dynamic nature of the covalent bonds follows an associative exchange mechanism, a unique feature of vitrimers, making the networks malleable and reshapable [24]. The ability to process materials with such properties via DLP 3D printing offers significant opportunities, for example, in creating soft robotic structures [25]. The presence of functional hydroxyl groups improves wettability and adhesion, allowing for potential surface functionalisation in reactions involving these groups [26].

In previous work, our group demonstrated that DBN is an efficient catalyst for accelerating thermo-activated transesterification reactions in dynamic thiol-epoxy networks [20]. In this follow-up study, we show that the dynamic properties can also be introduced in 3D-processable thiol-epoxy photopolymers by finding a good balance between cure kinetics and storage stability of the resins. This provides the possibility to process thiol-epoxy systems with a high degree of design freedom and additional functions based on the dynamic nature of the ester and -OH moieties present in the photopolymer.

2. Experimental

2.1. Materials

3,4-epoxycyclohexylmethyl-3′,4′-epoxycyclohexane carboxylate (ECC), bisphenol A diglycidyl ether (DGEBA), and 1-(2,4-dimethylphenylazo)-2-naphthol (Sudan II), used as a photoabsorber to increase the resolution during DLP 3D printing, were purchased from Sigma Aldrich (St. Louis, USA). The crosslinking agent pentaerythritol-tetrakis (3-mercaptopropionate) (PETMP) was obtained from Bruno Bock GmbH (Marschacht, Germany). 2-isopropylthioxanthone (ITX) was used as a photosensitiser and supplied by TCI (Tokyo, Japan). 1-Benzyl-3,4,6,7,8,8a-hexahydro-2H-pyrrolo[1,2-*a*]pyrimidine (trade name SCD-PLB-090) was used as a photolatent base and was kindly provided by SCD Dr. Sommerlade Chemistry Design GmbH (Neuenburg am Rhein, Germany). All chemicals were used as received, and their structures are shown in (Fig. 2).

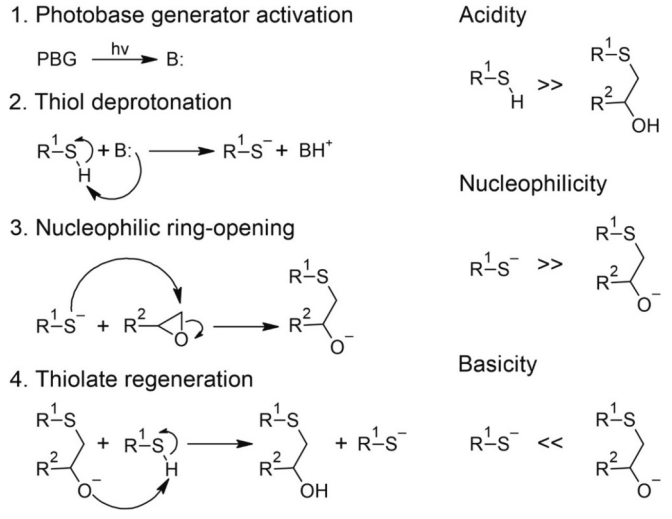

Fig. 1. The mechanism of the nucleophilic ring-opening reaction of epoxides in the presence of thiols, redrawn from Ref. [19] (PBG corresponds to the photobase generator and B: to the activated base).

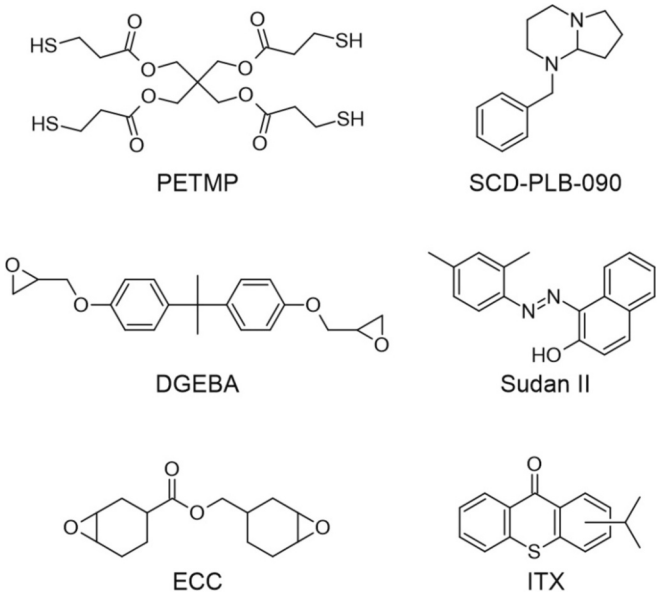

Fig. 2. Chemical structures of the compounds used in this study.

2.2. Preparation of resin formulations

For the sample preparation, SCD-PLB-090, ITX, and Sudan II were placed in light-protected vials and dissolved in the epoxy resin (either ECC or DGEBA). The formulations were mixed with a magnetic stirrer (300 rpm) at 50 °C for 30 min. Subsequently, the mixtures were cooled to room temperature, and PETMP was added in a stoichiometric amount of thiol groups relative to the epoxide groups. This was followed by 15 min of stirring and an ultrasonication step for another 15 min at room temperature. The compositions of the resin formulations under investigation are summarised in (Table 1).

2.3. Characterisation of resins

Rheological experiments were performed using an MCR 501 rheometer (Anton Paar, Austria). The viscosity measurements were carried out in rotation mode with a shear rate of 300 s^{-1}. The distance between the rotating disc and the base was set at 100 μm. Tests were conducted between 25 and 70 °C. The same setup in oscillation mode was used to detect the gel point. The oscillation value was 10 % of a full rotation, the frequency was 1 Hz, and the sample gap was 100 μm. During this test, the resin was illuminated with light from an Omnicure S2000 UV lamp without additional light filters and with a power density of 35 mW/cm^2 for 15 min.

The conversion of the resin components was monitored using FTIR spectroscopy on a Vertex 70 spectrometer (Bruker, USA). The measurements were carried out in the range of 4000–950 cm^{-1} with a spectral resolution of 4 cm^{-1}. For sample preparation, 10 μL of the resin was placed between two CaF_2 discs, and the depletion of the functional groups was followed upon visible light exposure with an LED lamp (Opsytec Dr. Groebel LED Control 5S) with a power density of 35 mW cm^{-2} ($\lambda = 405$ nm). For the kinetics studies at elevated temperature, the coated discs were heated on a hot plate. Once 50 °C was reached, the sample was irradiated with the LED lamp for 4 min, and an FTIR spectrum was taken. These steps were repeated until no further changes were observed in the obtained FTIR spectra. Using SpectraGryph software, peak areas in the regions of 2567 cm^{-1} (-SH groups), 1595 cm^{-1} (C—N bond), and 1737 cm^{-1} (C═O non-reacting ester groups in the thiol resin used, as internal reference) were calculated. From these data, the conversion of the PBG was calculated using Eq. (1), and the conversion of the PETMP was calculated using Eq. (2), according to the work of Bergoglio et al. [27].

$$\text{PBG conversion}(\%) = \left(1 - \frac{\left(\frac{A_{1595\ cm^{-1}}}{A_{1737\ cm^{-1}}}\right)_t}{\left(\frac{A_{1595\ cm^{-1}}}{A_{1737\ cm^{-1}}}\right)_{t=0}}\right) \times 100\% \quad (1)$$

$$\text{Thiol conversion}(\%) = \left(1 - \frac{\left(\frac{A_{2567\ cm^{-1}}}{A_{1737\ cm^{-1}}}\right)_t}{\left(\frac{A_{2567\ cm^{-1}}}{A_{1737\ cm^{-1}}}\right)_{t=0}}\right) \times 100\% \quad (2)$$

where A_x is the area of the corresponding peak at the selected measurement time and $t = 0$ corresponds to the first measurement.

Photo-DSC measurements were carried out on a NETZSCH Photo-DSC 204 F1 Phoenix (Germany) equipped with an Omnicure S2000 UV Lamp with a cut-off filter between 400 and 500 nm as the light source. Samples of 10 mg ± 0.1 mg were analysed in open aluminium crucibles. The samples were illuminated with a power density of 35 mW/cm^2 for 15 min. Measurements were carried out isothermally at 100, 90, 80, 70, and 60 °C under a nitrogen flow of 20 mL/min.

Table 1
Composition of tested resins.

Formulation ID	Epoxy momoner	SCD-PLB-090 (wt%)	ITX (wt%)	Sudan II (wt%)
DGEBA-8	DGEBA	8	2	0.1
ECC-8	ECC	8	2	0.1
ECC-5	ECC	5	2	0.1
ECC-2	ECC	2	2	0.1

2.4. DLP 3D printing

DLP 3D printing was carried out on a "Doppio" 3D printer prototype (W2P Engineering GmbH, Austria). The printer was equipped with an LED light engine from In-Vision Digital Imaging Optics GmbH with a pixel size of 50 μm, a wavelength of 405 nm, and an intensity of 35 mW/cm^2. Printing was conducted at 50 °C. After printing, all samples were post-treated in a Form Cure lamp (Formlabs, Netherlands) at 50 °C.

For bottom exposure tests, nine discs with a diameter of 1 cm were printed at varying irradiation times. The thickness of the previously cleaned and dried discs was then measured using a micrometre gauge. Three measurements were taken for each series, and the arithmetic average was calculated. To test the accuracy of the print, three identical objects were printed with different individual layer thicknesses of 25, 50 and 100 μm respectively. All printed objects were gently cleaned with isopropanol.

To determine the thermal stability of the photopolymers, thermogravimetric analysis was carried out on a TGA/DSC3+ (Mettler Toledo GmbH, Switzerland). The measurements were performed under a nitrogen atmosphere in a temperature range from 30 °C to 900 °C with a heating rate of 10 °C/min.

Dynamic mechanical analysis of DLP 3D-printed test specimens (35 mm × 0.5 mm × 22 mm) was carried out using a dynamic mechanical analyser DMA/SDTA861e (Mettler-Toledo, Switzerland). The experiments were performed in a nitrogen atmosphere over a temperature range from −30 °C to 150 °C with a heating rate of 3 °C/min. The frequency was set at 1 Hz, the maximum displacement was 3 μm, and the maximum force was 8 N. The glass transition temperature (Tg) was determined by the temperature at the maximum of the loss factor.

Stress relaxation measurements of DLP 3D-printed samples (discs with a diameter of 10 mm and a thickness of 0.3 mm) were carried out using a Physica MCR 501 rheometer (Anton Paar, Austria). The tests were performed with a plate-to-plate geometry, a torque strain of 3 %, and a normal force of 10 N, between 150 and 180 °C.

A shape programming experiment was performed to demonstrate the shape memory properties of the photopolymers. For this purpose, two samples (55 mm × 8 mm × 1 mm) were DLP 3D-printed. One of the test specimen was heated to 80 °C, bent in half, and cooled to room temperature maintaining its new shape. The other one was heated to 150 °C, bent in half, and kept in this new position for 30 min. After this time, the sample was cooled to room temperature maintaining its new shape. Both samples were then heated to 80 °C, and the shape changes were visually monitored.

3. Results and discussion

3.1. Reactivity and stability of thiol-epoxy resins

For the design of a resin formulation processable by DLP 3D printing, various key properties such as cure kinetics, viscosity, and storage stability must be considered [28]. In the first step, resin mixtures with a stoichiometric concentration of PEMTP and ECC were prepared (the molar ratio between epoxy and thiol groups was 1:1) with varying concentrations of SCD-PLB-090 as a photobase generator. In its inactive state, SCD-PLB-090 has a pKa value of 7.4, which shifts to 13.4, once DBN is liberated upon irradiation with UV light. DBN, as a strong base, is then able to efficiently catalyse the ring-opening reaction between epoxy and thiol moieties [29,30]. To shift the absorption window to the visible light spectral region and to obtain a good match with the emitting

light (405 nm) of the printer's light engine, isopropylthioxanthone (ITX) was added as a photosensitiser [18]. In all formulations, the ITX content was kept constant at 2 wt% to ensure a comparable transparency of the resin formulations in the visible light region [22,23]. In general, the ECC-based resin mixtures had a low viscosity of 60 mPa·s, making them ideal candidates for DLP 3D printing.

The curing kinetics as a function of the SCD-PLB-090 concentration (2–8 wt%) were studied upon light irradiation at 405 nm using FTIR spectroscopy. The related FTIR spectra are provided in the supporting information **(Fig. S1a-S1i)**. During the curing reaction, the IR signal corresponding to the characteristic thiol groups at 2567 cm^{-1} decrease, on the other hand the signal at 3500 cm^{-1} associated with -OH groups arose. Due to an overlapping of peaks in the region of 800–900 cm^{-1}, the decrease of the epoxy groups could not be followed quantitatively. Thus, the normalised IR band of the thiol groups was plotted versus curing time to evaluate the cure kinetics at room temperature (Fig. 3b**)**. A peak appeared at 1665 cm^{-1}, which is assigned to the formed C═N group of the released DBN, confirming the photoactivation of the catalyst. In addition, the photo-triggered liberation of DBN was observed by the disappearing peaks at 1640 and 1595 cm^{-1}, which are related to the subtraction of hydrogen from the C—H group in the 6-position of 1-benzyl-3,4,6,7,8,8a-hexahydro-2H-pyrrolo[1,2-*a*]pyrimidine, and the cleavage of the C—N bond of the protective group during the formation of DBN, respectively. The peak at 1595 cm^{-1} was chosen to calculate the catalyst conversion because its base is flat and thus gives less error at high conversion. Fig. 3a shows the catalyst conversion in ECC-8 versus exposure time.

Comparing the decrease of the -SH (ring-opening reaction) and the decrease of C—N bands at 1595 cm^{-1} (related to the release of DBN), the experiment revealed that the activation of the catalyst occurs within considerably shorter illumination times than the curing of the thiol and epoxy monomers. The intensity of the C—N signal remained constant (indicating maximum release of DBN) after 3 min of light exposure. Once the maximum release of the catalyst was obtained, the lamp was switched off, and it took more than three hours to reach a final thiol conversion of over 90 % under dark conditions. Interestingly, the effect of the PBG concentration on the cure rate and final monomer conversion was negligible (**Fig. S1j**).

Based on tests with varying amounts of catalyst, we conclude that in thin films a higher content of the photolatent base does not slow down the formation of catalysing species due to an inner filter effect as the ITX conent was kept constant in the three formulations. On the other hand, the results suggest that the low rate of the curing reaction (at room temperature) cannot be significantly accelerated by a higher number of DBN molecules in the system. As the release of the catalyst and the number of catalysing species were not the rate-limiting steps of the curing reaction, the reaction temperature was gradually increased. Resin ECC-8 was chosen for further studies to ensure a sufficient amount of DBN present in the thiol-epoxy network for subsequently catalysing bond exchange reactions at elevated temperatures (required for the reshaping of printed parts). In the first step, the FTIR experiment was repeated at 50 °C. The higher temperature considerably accelerated the ring-opening reaction, and a monomer conversion >90 % was already obtained within 40 min, whilst the thiol conversion amounted to 10 % after 4 min of light exposure.

Photo-DSC analysis was additionally performed to determine the heat enthalpy of the curing reaction (Fig. 4a**)**. It should be noted that a different light source was used (a medium-pressure mercury emitter with a 400–500 nm cut-off filter) compared to the previously described FTIR studies. At 50 °C, it was not possible to follow any curing reaction as the evolved reaction heat was too low to be measured. At 60 °C, a very broad curve was observed, which is typical for curing reactions suffering from delayed monomer conversion. By raising the temperature from 60 to 100 °C, the increase in reactivity was clearly demonstrated by the shift in the time needed to reach the maximum heat flow from 10 min to 1 min. At the same time, the maximum heat flow increased from 0.68 to 3.98 mW/mg (Fig. 4a**)**. The heat of the reaction obtained at 80 and 100 °C amounted to 473 and 466 J/g, respectively. Between 70 and 90 °C, the curves still showed a pronounced tailing caused by the delayed step-growth reaction between thiol and epoxy groups. At 100 °C, the tailing disappeared, and the cure kinetics were comparable to some radical-mediated thiol-ene systems reported in literature [31]. The conversion of monomers calculated based on DSC analysis is in good agreement with the results of FTIR analysis (Fig. 4b**)**.

While a higher temperature is beneficial for accelerating the cure kinetics, it poses several challenges when it comes to the 3D printing of thiol-epoxy resins. The applicable temperature is limited by the evaporation of volatile monomers during printing and the hardware of the printer. With the printer used in this study, the vat could be heated to a maximum temperature of 65 °C. However, in the thiol-epoxy resins under investigation, the major issue was the poor storage stability of the resin. Althought resin ECC-8 was stable over several days at room temperature, it started gelling at temperatures above 70 °C, even under dark conditions. This is related to basic impurities catalysing the chain reaction of curing. Moreover, SCD-PLB-090 carries tertiary amino groups in its inactive state, which are also able to catalyse the curing reaction at elevated temperatures [32].

To evaluate the storage stability of the thiol-epoxy resin, rheological studies were carried out on resin ECC-8, which was kept at different temperatures, and the change in viscosity was monitored under dark conditions (Fig. 5a**)**. At 50 °C, the resin remained stable for at least 6 h, which makes the 3D printing of objects feasible. At 60 and 70 °C,

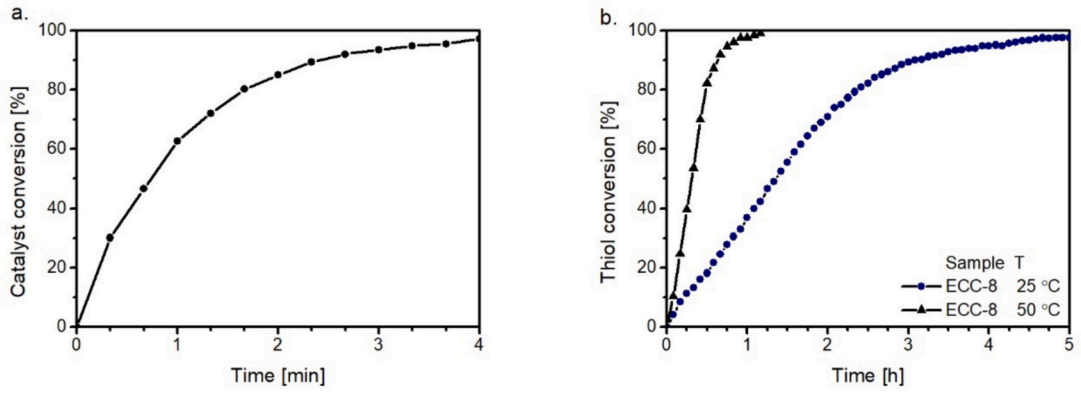

Fig. 3. (a) Monitoring the release of the catalyst over irradiation time (405 nm), following the decrease of the normalised C—H peak at 1640 cm^{-1} on resin ECC-8 and (b) following the normalised -SH absorption band at 2567 cm^{-1} over irradiation time (405 nm) to determine the thiol conversion. The irradiation was carried out at 25 and 50 °C.

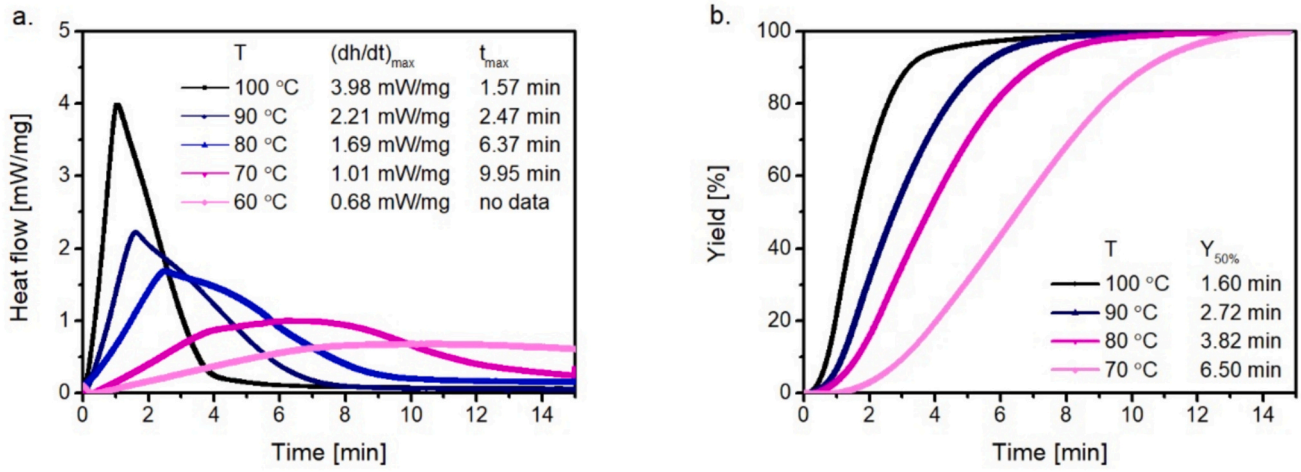

Fig. 4. Photo-DSC curves on resin ECC-8: (a) Evolution of the heat release achieved at different temperatures during visible light irradiation and (b) reaction yield based on heat flow integration.

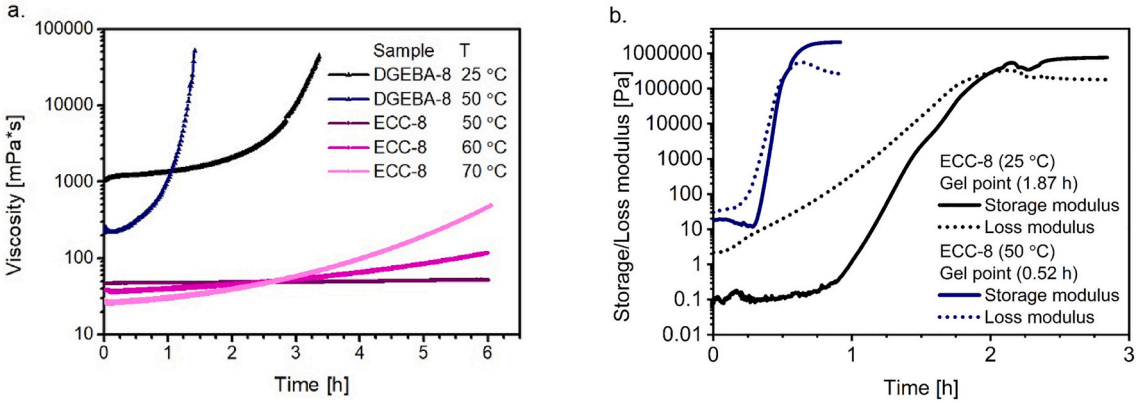

Fig. 5. Rheological data on studied resins: (a) Monitoring the viscosity over time at different temperatures and (b) change in storage and loss modulus upon visible light irradiation at 25 and 50 °C for resin ECC-8.

prepolymerisation of the resin commenced after 3 h under dark conditions, and the viscosity steadily increased after 6 h. Repeating the experiment under simultaneous visible light irradiation showed a distinctive increase in storage and loss modulus related to the photo-induced curing reaction (Fig. 5b).

Unsurprisingly, by increasing the temperature from 25 to 50 °C, the light-induced increase in the modulus is sharper and occurs within a shorter time, which is in good agreement with the photo-DSC and FTIR data. However, even at 50 °C, the gel point is reached only after 31 min. In further rheological studies, ECC was replaced with the more reactive and higher viscous DGEBA resin (DGEBA-8). While the resin had a higher viscosity (210 mPa·s), premature gelation was observed at 50 °C, with the viscosity drastically increased after 20 min. At room temperature, the resin remained only stable for 2 h, which is insufficient for any DLP 3D printing application.

3.2. DLP 3D-printing with thiol-epoxy resins

All subsequent 3D printing experiments were conducted with ECC-8 at 50 °C. Although the cure kinetics were significantly slower than typical radical-mediated resin systems used in vat photopolymerisation 3D printing, the resin provided sufficiently high storage stability at 50 °C and benefited from a low viscosity. To evaluate the influence of the cure kinetics on the printability, bottom exposure tests were performed to determine the minimum exposure time and thickness of a single printed layer. For this purpose, the discs were printed with different exposure times at 405 nm (35 mW/cm^2) and their thickness was then measured. Based on FTIR kinetics studies, it is known that the theoretical minimum exposure time required for maximum activation of the catalyst under the test conditions is approximately 3 min. Based on photo-rheology, the time to reach the gel point was determined to be 31 min. Therefore, in the first test, 9 discs were exposed between 80 and 240 s, increasing the exposure time for each subsequent disc by 20 s, and then leaving the discs in the vat without exposure for 30 min to complete dark curing. Images of the cured discs are illustrated in Fig. 6a. The graphic shows that all discs were successfully cured, but the two discs with the shortest exposure time could not be removed from the vat because they were too thin. The related Jacobs working curve is provided in Fig. 6b, which clearly shows that the discs' thickness increases with rising exposure time. Based on the logarithmic curve fitting ($R^2 = 0.9517$), the calculated minimum exposure time for a single layer is 44 s, and the minimum energy dose is 1.54 J/cm^2. These data and previous experiments allow us to assume that this corresponds to a 45 % conversion of the catalyst. Which means that the solidification of the discs occurs even though the catalyst is not fully activated. This confirms the results of the previous data showing that - at a high concentration of the PBG (8 wt%) - the limiting factor is the rate of chain reaction between the thiolate and the epoxide (**Fig. S1j**).

Bottom exposure tests were repeated with resins containing a lower amount of catalyst to assess the effect of the catalyst concentration on

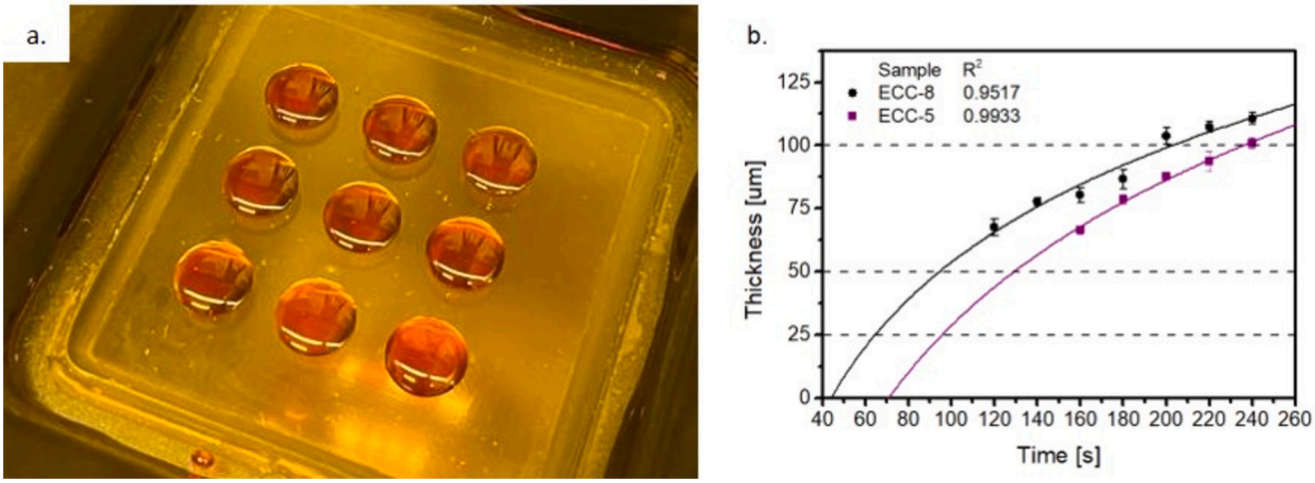

Fig. 6. (a) Photograph of discs (d = 1 cm) printed during the bottom exposure test of resin ECC-8 and (b) distribution of the discs' thickness versus exposure time. After light exposure, the thickness of the discs was measured after 30 min at 50 °C.

the thickness of the cured layer. For a sample containing 2 wt% of catalyst (ECC-2), the discs did not solidify. In the presence of 5 wt% catalyst (ECC-5), the discs were successfully cured, and the results are provided in Fig. 6b. Here, only 5 discs could be removed from the build platform, and their thickness was lower compared to the samples obtained with resin ECC-8. Based on the results, it can be concluded that the amount of catalyst does not accelerate the reaction, but its concentration affects the initiation of the chain reaction in the deeper regions of the resin layer. This phenomenon was not observed during photo-DSC and FTIR tests as the thickness of the sample was significantly lower and the effect of catalyst concentration was not detectable. Based on the results further printing experiments were carried out with ECC-8 using an exposure time of 5 min and 25 mW/cm^2. Such parameters should lead to the full activation of the catalyst needed for the dynamic exchange of bonds in later tests when reducing light intensity should mitigate the negative impact of scattered light.

In the next step, the influence of the dark curing reaction was determined. For this purpose, the layer was exposed to light for 5 min and then left for defined times. The shortest waiting time at which it was possible to obtain a solid disc was 15 min, which, together with the exposure time of 5 min, gives a layer printing time of 20 min. The determined time coincides with the results of photo-rheology, where a visible increase in modulus occurred 20 min after the start of light exposure. Then, the printing platform was lowered to a height of 100, 50, and 25 μm to determine if the disc cured within the minimum determined time would attach to the platform. The test was successful for all single-layer thicknesses under investigation. Further experiments confirmed that it is possible to cure another layer on the first one using these parameters. When a new layer is printed, the previous layer has time to complete dark curing. This shortened the time needed to cure a 100 μm layer from 31 min to 20 min. Based on the tests performed, 20 min was determined as the minimum total time required to cure a 100 μm thick layer under the applied conditions (50 °C, 25 mW/cm^2) for resin ECC-8.

To determine the printing resolution, a comb-like object with teeth varying in width and distance was printed. A model of the printed object and its dimensions are shown in **Fig. S2a**. To investigate the effect of printing speed on accuracy, three identical objects were printed with the same irradiation time per layer but differing in layer thickness, which amounted to 25, 50, and 100 μm. Photographs of the printed model objects are provided in **Figs. S2b** and **S2c**. Even thought all three objects were successfully printed, the speed of printing and the power of light had a significant impact on the accuracy of the print, as can be seen in the photographs **(Fig. S2)**. The structure printed with a layer thickness of 100 μm had the highest accuracy. The lower layer thickness (and prolonged exposure time) favoured the formation of over-cured regions at the edges of the printed structures, compromising on the printing resolution. As a Sudan dye was added as a photo absorber, this effect is not expected to be caused by light scattering but by the migration of the unbound, active catalyst to the non-exposed areas. This is particularly facilitated by the elevated temperature of the vat and the low viscosity of the resin. The chain reaction between thiol and epoxide can proceed and activate the monomers beyond the region of light. This process is influenced primarily by the mobility of the components, which is related to the possibility of migration of active ingredients.

To demonstrate the capability of printing more complex (in x,y-direction) structures, rectangular-shaped objects with inscribed logos were DLP 3D printed with a single layer thickness of 100 μm, using 5 min of irradiation and 15 min of dark-curing time per layer. Despite some unevenness on the surface and partial over-curing, all details of the logos were successfully reproduced. This can be observed by comparing the 3D model of the logos shown in Fig. 7a with the photograph of the print provided in Fig. 7b. Fig. 7c presents a microscopic image at ten times magnification, highlighting the smallest printed letters. Although the build speed was quite slow, this experiment serves as a proof of concept for the applicability of the tested resin in DLP technology.

Alongside the optimisation of printing parameters, the ageing of the resin was investigated. For this purpose, the resin from the vat (after printing at 50 °C for 6 h) was collected and placed in a refrigerator at 0 °C. The change in viscosity was monitored over 7 days using rheology, and the shelf life of the resin "after printing" was compared to that of a freshly prepared batch of resin, which was stored either at 25 °C or 0 °C (Fig. 8a). At 0 °C, the freshly prepared sample remained stable for 14 days, with a negligible increase in viscosity. At 25 °C, however, the resin exhibited a reduced stability, with a noticeable rise in viscosity after 7 days. In contrast, the increase in viscosity of the uncured resin collected post-printing was considerably more pronounced, reaching 6 Pa·s after two weeks of storage in the fridge.

This behaviour is primarily attributed to the migration of liberated DBN to the non-exposed areas of the resin during printing, which induced partial pre-curing of the resin. This pre-curing process continued during storage in the presence of alkaline species. This was corroborated by FTIR spectroscopy, which showed a decrease in the thiol signal (2567 cm^{-1}) and an increase in the -OH band (3500 cm^{-1}) during storage (Fig. 8b). It should be noted that these viscosity measurements were performed at 25 °C, whilst the printing was conducted at 50 °C. At 50 °C, the viscosity of the aged resin amounted to 90 mPa·s, which still permitted the printing of the recovered resin after two weeks

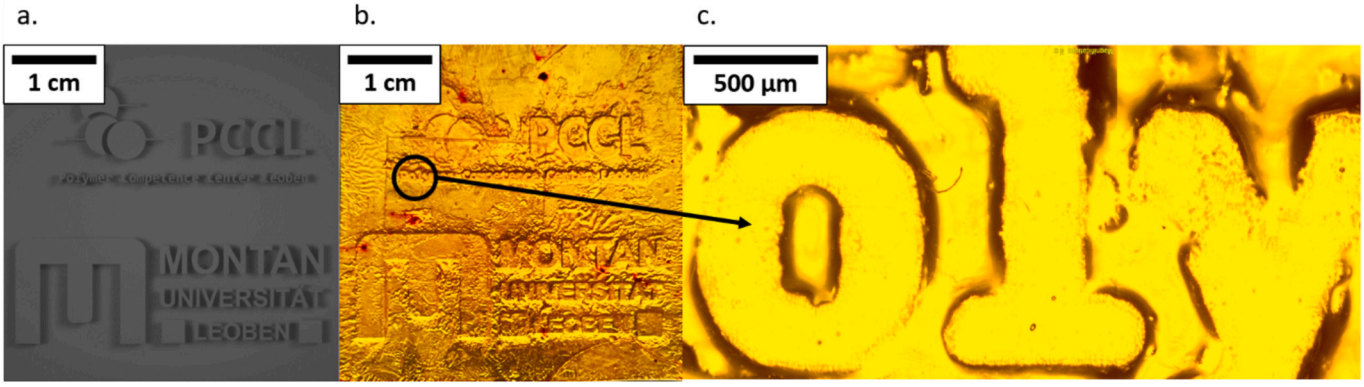

Fig. 7. (a) 3D model and (b) photograph of printed logos on free-standing object. (c) Optical micrograph of the printed logo with 10-fold magnification.

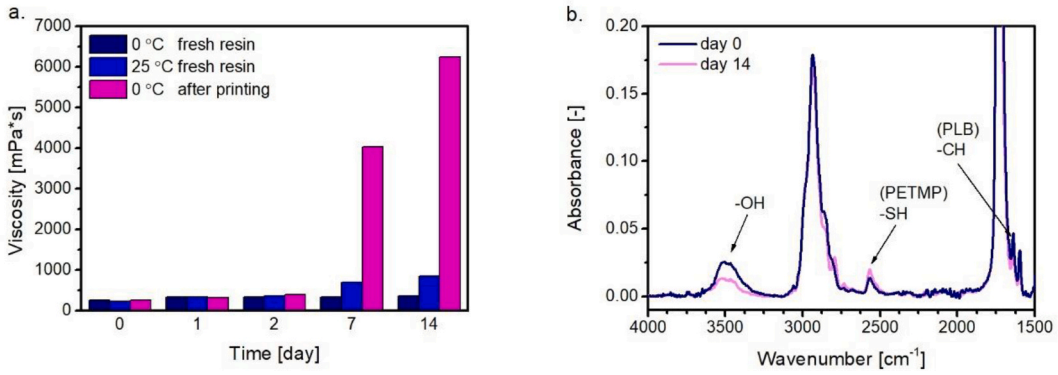

Fig. 8. (a) Change in the viscosity (resin ECC-8) over time as a function of storage temperature. (b) FTIR spectra of resin ECC-8 (recovered after printing) prior to and after storage for 14 days at 0 °C.

of storage. For a proof-of-concept, the resin recovered after printing and stored for two weeks at 0 °C was used to reprint the logo by applying the same printing parameters as for the fresh resin. All features were reproduced successfully (**Fig. S3a**) but the resolution of the letters was negatively affected by overpolymerization (**Fig. S3b**). The results suggest that the pregelation of the resin compromises on the quality of the printed object whilst the stability of the resin is still sufficiently high for DLP 3D printing.

Despite efforts to optimise the composition of the thiol-epoxy resin and to adjust the printing parameters, its performance remained inferior to that of acrylate, epoxy, or thiol-acrylate based resins reported in the literature. The most significant drawback is the print speed, which was 5 µm/min for ECC-8, compared to >1 cm/min for other reported photocurable systems [13,34,35]. In addition, migration of the catalysing species negatively affected the resolution of the printed objects. However, with a feature size of 250 µm (x,y-direction) it is comparable to some other resins used in DLP 3D printing [36]. A key advantage of ECC-8 is its stability compared to other thiol-epoxy-based systems [7,11]. Summing up, the 3D printability of photo-curable epoxy-thiol resins has been confirmed, but further work is required to increase the print speed and to minimise overcuring.

3.3. *Thermomechanical and dynamic properties of 3D-printed objects*

TGA, DSC and DMA analysis was carried out to study the thermomechanical properties of the DLP 3D-printed objects. DSC curves revealed that the glass transition temperature (Tg) shifts from 52 °C to 61 °C in the second heating run (**Fig. S4**), which indicates incomplete conversion of the monomers during printing. Thus, the 3D-printed objects were post-baked at 180 °C for 1 h and TGA curves of the samples were taken prior to and after thermal post-curing. The printed samples show a significant weight loss (2 %) between 100 and 200 °C attributed to humidity (due to its high polarity the network is prone to water uptake) and unreacted monomers (**Fig. S5a**). After post-baking, the mass loss is signficantly lower but the release of water is still observable as the post-treated sample was measured after storing it for 7 months at room temperature. However, independent of the thermal post-baking step, the main mass loss related to the degradation of the polymer network started at ~250 °C (**Fig. S5b**). Based on these results, it can be concluded that the samples can be safely handled at temperatures up to 180 °C. The Tg of the printed ECC-8 and post-cured sample was confirmed by dynamic mechanical analysis (DMA). Only a single peak with a relatively narrow width was observed in the tan(δ) curve **(Fig. S6)**. This suggests a homogeneous network structure, which is characteristic of thiol-click photopolymers. A Tg above room temperature is advantageous for conducting shape memory experiments on 3D-printed structures.

The cured photopolymer contained a significant number of ester groups (from both thiol and epoxy monomers) and free -OH groups (resulting from the ring-opening of the epoxy groups), which are capable of undergoing bond exchange reactions at elevated temperature. Since the photo-activated DBN molecules are not consumed during the curing reaction, they can be utilised as catalysts to accelerate transesterification reactions. To monitor the kinetics of these bond exchange reactions, stress relaxation experiments were conducted on DLP 3D-printed test specimens at varying temperatures.

A temperature range of 150 to 180 °C was selected, which is well above the Tg but below the degradation temperature of the ECC-8 photopolymer. (Fig. 9a) illustrates the time-dependent evolution of the relaxation modulus. The stress relaxation exhibits a clear temperature dependence, indicating an increasing bond exchange rate with rising temperature. This behaviour is typical of dynamic polymer networks that rely on an associative bond exchange mechanism. By

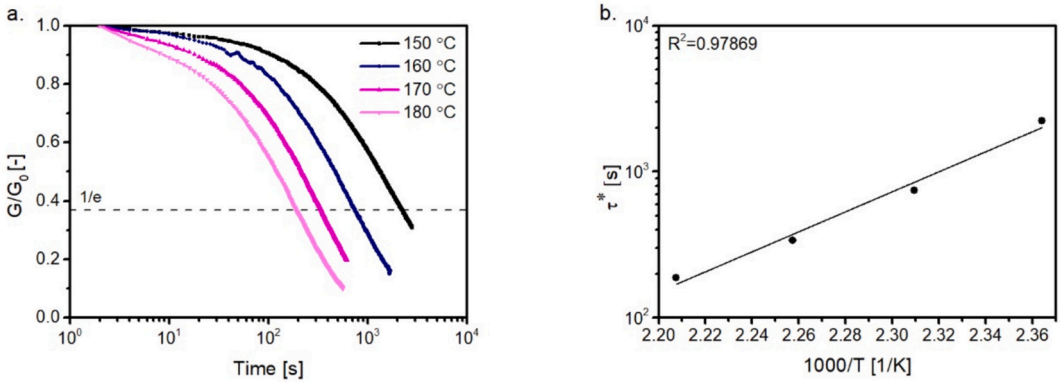

Fig. 9. (a) Stress relaxation of the cured thiol-epoxy network as a function of time and temperature; (b) Arrhenius plot as obtained from the stress relaxation data.

employing the Maxwell model, the characteristic relaxation times (τ*) were determined, representing the time required for the network to relax to 1/e of its initial stress at the applied temperatures [33]. Fig. 9b shows that the data conform to the Arrhenius law, thereby confirming the associative nature of the bond exchange reactions in the photopolymer.

In a final experiment, the bond exchange reactions and associated temperature-induced topological rearrangements were utilised to permanently reshape DLP 3D-printed objects. For this purpose, printed rectangular test bars were deformed into a U-shape between two metal blocks at two different temperatures (Fig. 10). In the first experiment, a sample was heated to 80 °C, which was above the network's Tg but below the temperature required to initiate bond exchange reactions. Upon cooling to room temperature, the deformed samples retained the programmed U-shape. However, when reheated to 80 °C, the sample reverted to its original rectangular form, demonstrating a behaviour characteristic of entropy-driven Tg-based shape memory polymers. In contrast, when the experiment was repeated at 150 °C (a temperature sufficiently high to induce bond exchange reactions as indicated by the stress relaxation experiments) a different outcome was observed. At this elevated temperature, the network structure was reorganised during deformation, and the reshaped structure was maintained even when the network was subsequently heated above its Tg. This capability for permanent reshaping exemplifies one of the many features of dynamic polymer networks. The integration of such features with the processability of 3D printing offers significant potential for future applications.

4. Conclusions

The present work demonstrates the feasibility of the photo-induced thiol-epoxy click reaction for fabricating objects via vat photopolymerization 3D printing. By optimising the resin formulation, a balance between cure rate and storage stability was obtained, which is crucial for the successful printing of 3D objects. However, even with the optimized resin, the build speed is significantly slower compared to radically cured systems. The cure reactions can be accelerated by increasing the temperature, but this compromises the resin's stability. Cycloaliphatic epoxide monomers (ECC) exhibit a higher stability than aromatic counterparts (DGEBA) and can be processed by DLP 3D printing at 50 °C. When stored at 0 °C, the resins remain stable for up to two weeks. Increasing the photobase concentration beyond 2 wt% does not affect the reaction rate but influences the thickness of the cured polymer layer. The photobase generator in this system serves a dual function: upon light activation, the released base (DBN) does not only catalyse the ring-opening reaction between thiol and epoxy groups but also thermally activates transesterification in the cured photopolymers. Thus, DLP 3D-printed objects with dynamic network properties can be printed, which paves the way towards the printing of devices with additional functions (e.g. healability). However, additional research has to be done to accelerate the cure rate and thus, the build speed, without negatively affecting the pot life of the resins.

CRediT authorship contribution statement

Szymon Gaca: Writing – original draft, Methodology, Investigation, Data curation. **Kurt Dietliker:** Writing – review & editing, Validation, Resources. **Elisabeth Rossegger:** Writing – review & editing, Validation, Methodology, Conceptualization. **Sandra Schlögl:** Writing – review & editing, Validation, Supervision, Project administration, Methodology, Investigation, Funding acquisition, Conceptualization.

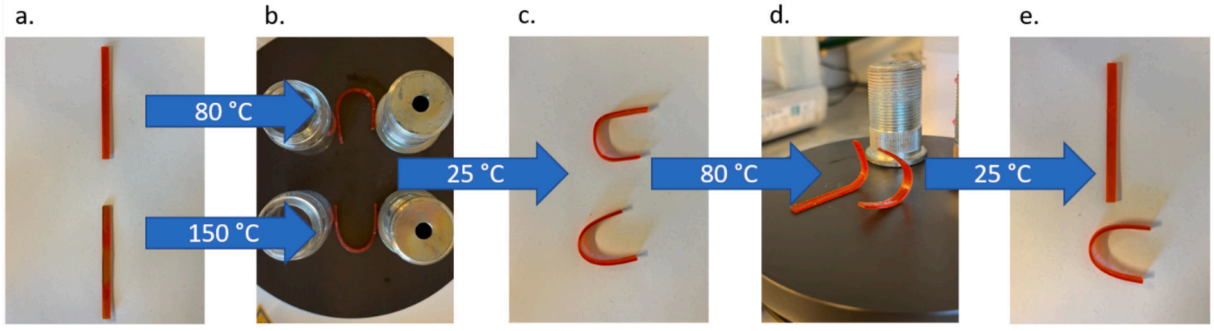

Fig. 10. (a) Printed test samples (55 mm × 8 mm × 1 mm). (b) One of the samples was heated to 80 °C and deformed into a bent shape. The other sample was heated to 150 °C and bent in the same way. (c) Both samples were kept in their programmed states for 30 min, then cooled to room temperature. (d) The programmed samples were reheated to 80 °C without applying any external stress. (e) After 5 min, the samples were cooled back to room temperature. The sample initially heated to 80 °C reverted to its original shape, whilst the sample initially heated to 150 °C retained its new shape.

Declaration of competing interest

The authors declare that they have no known competing financial interests or personal relationships that could have appeared to influence the work reported in this paper.

Acknowledgements

The research work was performed at the Polymer Competence Center Leoben GmbH (PCCL, Austria) within the #horizoneurope20212027 programme under the Marie Skłodowska-Curie Doctoral Networks (MSCA-DN) grant agreement No 101073432. Funding was provided by the European Union. Part of the research work was also carried out within the COMET-Module project "Repairtecture" (project-no.: 904927) at the Polymer Competence Center Leoben GmbH (PCCL, Austria) within the framework of the COMET-program of the Federal Ministry for Climate Action, Environment, Energy, Mobility, Innovation and Technology and the Federal Ministry of Labour and Economy. The PCCL is funded by the Austrian Government and the State Governments of Styria, Upper and Lower Austria. In addition, the authors thank Walter Alabiso (PCCL) for performing the DMA tests, Roman Korotkov (PCCL) for carrying out the DSC experiments and Mathias Kriehuber (PCCL) for performing the TGA measurements.

Appendix A. Supplementary data

Supplementary data to this article can be found online at https://doi.org/10.1016/j.reactfunctpolym.2024.106085.

Data availability

The raw/processed data required to reproduce the above findings cannot be shared at this time due to time limitations.

References

[1] S. Saleh Alghamdi, S. John, N. Roy Choudhury, N.K. Dutta, Additive manufacturing of polymer materials: progress, promise and challenges, Polymers 13 (2021), https://doi.org/10.3390/polym13050753.
[2] S.C. Ligon, R. Liska, J. Stampfl, M. Gurr, R. Mülhaupt, Polymers for 3D printing and customized additive manufacturing, Chem. Rev. 117 (2017) 10212–10290, https://doi.org/10.1021/acs.chemrev.7b00074.
[3] T. Hada, M. Kanazawa, N. Miyamoto, H. Liu, M. Iwaki, Y. Komagamine, S. Minakuchi, Effect of different filler contents and printing directions on the mechanical properties for photopolymer resins, Int. J. Mol. Sci. 23 (2022), https://doi.org/10.3390/ijms23042296.
[4] Y. Liu, Y. Lin, T. Jiao, G. Lu, J. Liu, Photocurable modification of inorganic fillers and their application in photopolymers for 3D printing, Polym. Chem. 10 (2019) 6350–6359, https://doi.org/10.1039/c9py01445d.
[5] I. Cazin, E. Rossegger, I. Roppolo, M. Sangermano, P. Granitzer, K. Rumpf, S. Schlögl, Digital light processing 3D printing of dynamic magneto-responsive thiol-acrylate composites, RSC Adv. 13 (2023) 17536–17544, https://doi.org/10.1039/d3ra02504g.
[6] S.D. Nath, S. Nilufar, An overview of additive manufacturing of polymers and associated composites, Polymers 12 (2020), https://doi.org/10.3390/polym12112719.
[7] E. Rossegger, R. Höller, K. Hrbinič, M. Sangermano, T. Griesser, S. Schlögl, 3D printing of soft magnetoactive devices with thiol-click photopolymer composites, Adv. Eng. Mater. 25 (2023), https://doi.org/10.1002/adem.202200749.
[8] A. Bagheri, J. Jin, Photopolymerization in 3D printing, ACS Appl. Polym. Mater. 1 (2019) 593–611, https://doi.org/10.1021/acsapm.8b00165.
[9] T. Jiang, Y. He, Y. Jian, J. Nie, Exploration for decreasing the volume shrinkage for photopolymerization, Prog. Org. Coat. 75 (2012) 398–403, https://doi.org/10.1016/j.porgcoat.2012.07.007.
[10] S.C. Ligon-Auer, M. Schwentenwein, C. Gorsche, J. Stampfl, R. Liska, Toughening of photo-curable polymer networks: a review, Polym. Chem. 7 (2016) 257–286, https://doi.org/10.1039/c5py01631b.
[11] L. Chen, Q. Wu, G. Wei, R. Liu, Z. Li, Highly stable thiol–ene systems: from their structure–property relationship to DLP 3D printing, J. Mater. Chem. C 6 (2018) 11561–11568, https://doi.org/10.1039/C8TC03389G.
[12] H. Leonards, S. Engelhardt, A. Hoffmann, L. Pongratz, S. Schriever, J. Bläsius, M. Wehner, A. Gillner, Advantages and drawbacks of thiol-ene based resins for 3D-printing, in: H. Helvajian, A. Piqué, M. Wegener, B. Gu (Eds.), Laser 3D Manufacturing II, SPIE, 2015, p. 93530F.
[13] U. Shaukat, B. Sölle, E. Rossegger, S. Rana, S. Schlögl, Vat Photopolymerization 3D-printing of dynamic thiol-acrylate photopolymers using bio-derived building blocks, Polymers 14 (2022), https://doi.org/10.3390/polym14245377.
[14] A. Oesterreicher, J. Wiener, M. Roth, A. Moser, R. Gmeiner, M. Edler, G. Pinter, T. Griesser, Tough and degradable photopolymers derived from alkyne monomers for 3D printing of biomedical materials, Polym. Chem. 7 (2016) 5169–5180, https://doi.org/10.1039/c6py01132b.
[15] Y. Wu, M.C. Simpson, J. Jin, 3D printing of thiol-Yne Photoresins through visible light Photoredox catalysis, ChemistrySelect 7 (2022), https://doi.org/10.1002/slct.202200319.
[16] I. Roppolo, F. Frascella, M. Gastaldi, M. Castellino, B. Ciubini, C. Barolo, L. Scaltrito, C. Nicosia, M. Zanetti, A. Chiappone, Thiol–yne chemistry for 3D printing: exploiting an off-stoichiometric route for selective functionalization of 3D objects, Polym. Chem. 10 (2019) 5950–5958, https://doi.org/10.1039/C9PY00962K.
[17] D. Hennen, D. Hartmann, P.H. Rieger, A. Oesterreicher, J. Wiener, F. Arbeiter, M. Feuchter, E. Fröhlich, M. Pichelmayer, S. Schlögl, T. Griesser, Exploiting the carbon and Oxa Michael addition reaction for the synthesis of Yne monomers: towards the conversion of acrylates to biocompatible building blocks, ChemPhotoChem 4 (2020) 476–480, https://doi.org/10.1002/cptc.201900199.
[18] B.D. Fairbanks, L.J. Macdougall, S. Mavila, J. Sinha, B.E. Kirkpatrick, K.S. Anseth, C.N. Bowman, Photoclick chemistry: a bright idea, Chem. Rev. 121 (2021) 6915–6990, https://doi.org/10.1021/acs.chemrev.0c01212.
[19] H. Yeo, A. Khan, Photoinduced proton-transfer polymerization: a practical synthetic tool for soft lithography applications, J. Am. Chem. Soc. 142 (2020) 3479–3488, https://doi.org/10.1021/jacs.9b11958.
[20] D. Reisinger, K. Dietliker, M. Sangermano, S. Schlögl, Streamlined concept towards spatially resolved photoactivation of dynamic transesterification in vitrimeric polymers by applying thermally stable photolatent bases, Polym. Chem. 13 (2022) 1169–1176, https://doi.org/10.1039/d1py01722e.
[21] M. Bouzrati-Zerelli, M. Frigoli, F. Dumur, B. Graff, J.P. Fouassier, J. Lalevée, Design of novel photobase generators upon violet LEDs and use in photopolymerization reactions, Polymer 124 (2017) 151–156, https://doi.org/10.1016/j.polymer.2017.07.068.
[22] L. Chen, Y. Zheng, X. Meng, G. Wei, K. Dietliker, Z. Li, Delayed thiol-epoxy Photopolymerization: a general and effective strategy to prepare thick composites, ACS Omega 5 (2020) 15192–15201, https://doi.org/10.1021/acsomega.0c01170.
[23] Y. Jian, Y. He, Y. Sun, H. Yang, W. Yang, J. Nie, Thiol–epoxy/thiol–acrylate hybrid materials synthesized by photopolymerization, J. Mater. Chem. C 1 (2013) 4481, https://doi.org/10.1039/c3tc30360h.
[24] V. Bijalwan, S. Rana, G.J. Yun, K.P. Singh, M. Jamil, S. Schlögl, 3D printing of covalent adaptable networks: overview, applications and future prospects, Polym. Rev. 64 (2024) 36–79, https://doi.org/10.1080/15583724.2023.2227692.
[25] S. Terryn, J. Langenbach, E. Roels, J. Brancart, C. Bakkali-Hassani, Q.-A. Poutrel, A. Georgopoulou, T. George Thuruthel, A. Safaei, P. Ferrentino, T. Sebastian, S. Norvez, F. Iida, A.W. Bosman, F. Tournilhac, F. Clemens, G. van Assche, B. Vanderborght, A review on self-healing polymers for soft robotics, Mater. Today 47 (2021) 187–205, https://doi.org/10.1016/j.mattod.2021.01.009.
[26] L. Shahzadi, F. Maya, M.C. Breadmore, S.C. Thickett, Functional materials for DLP-SLA 3D printing using thiol–acrylate chemistry: resin design and postprint applications, ACS Appl. Polym. Mater. 4 (2022) 3896–3907, https://doi.org/10.1021/acsapm.2c00358#.
[27] M. Bergoglio, Z. Najmi, A. Cochis, M. Miola, E. Vernè, M. Sangermano, UV-cured bio-based Acrylated soybean oil scaffold reinforced with bioactive glasses, Polymers 15 (2023), https://doi.org/10.3390/polym15204089.
[28] L. Strohmeier, H. Frommwald, S. Schlögl, Digital light processing 3D printing of modified liquid isoprene rubber using thiol-click chemistry, RSC Adv. 10 (2020) 23607–23614, https://doi.org/10.1039/D0RA04186F.
[29] K. Dietliker, R. Hüsler, J.-L. Birbaum, S. Ilg, S. Villeneuve, K. Studer, T. Jung, J. Benkhoff, H. Kura, A. Matsumoto, H. Oka, Advancements in photoinitiators—opening up new applications for radiation curing, Prog. Org. Coat. 58 (2007) 146–157, https://doi.org/10.1016/j.porgcoat.2006.08.021.
[30] M. Sangermano, A. Vitale, K. Dietliker, Photolatent amines producing a strong base as photocatalyst for the in-situ preparation of organic–inorganic hybrid coatings, Polymer 55 (2014) 1628–1635, https://doi.org/10.1016/j.polymer.2014.02.045.
[31] E. Rossegger, Y. Li, H. Frommwald, S. Schlögl, Vat photopolymerization 3D printing with light-responsive thiol-norbornene photopolymers, Monatsh. Chem. 154 (2023) 473–480, https://doi.org/10.1007/s00706-022-03016-5.
[32] A. Romano, I. Roppolo, M. Giebler, K. Dietliker, Š. Možina, P. Šket, Stimuli-responsive thiol-epoxy networks with photo-switchable bulk and surface properties, RSC Adv. 8 (73) (2018) 41904–41914, https://doi.org/10.1039/c8ra08937j.
[33] M. Capelot, M.M. Unterlass, F. Tournilhac, L. Leibler, Catalytic control of the Vitrimer glass transition, ACS Macro Lett. 1 (2012) 789–792, https://doi.org/10.1021/mz300239f.
[34] I. Cazin, M. Ocepek, J. Kecelj, A.S. Stražar, S. Schlögl, Synthesis of bio-based polyester resins for vat Photopolymerization 3D printing, Materials (Basel) 17 (2024), https://doi.org/10.3390/ma17081890.
[35] M. Bergoglio, E. Rossegger, S. Schlögl, T. Griesser, C. Waly, F. Arbeiter, M. Sangermano, Multi-material 3D printing of biobased epoxy resins, Polymers (Basel) 16 (2024), https://doi.org/10.3390/polym16111510.
[36] J. Borrello, P. Nasser, J. Iatridis, K.D. Costa, 3D printing a mechanically-tunable acrylate resin on a commercial DLP-SLA printer, Addit. Manuf. 23 (2018) 374–380, https://doi.org/10.1016/j.addma.2018.08.019.